Numerical Study of Free Liquid Jet Primary Breakup Phenomenon in Still Gases

Ahmed Dahia[1], Faiza Zidouni[2], Amine Boualouache[2], Amina Lyria Cheridi[1], Amel Dadda[1]

[1]Nucear Rsearch Centre of Birine, B.P 180 Ain Oussera 17200, Djelfa, Algeria
[2]Laboratory of Theoretical and Applied Fluid Mechanics, Faculty of Physics, USTHB, Bab Ezzouar, Algeria
[*]Corresponding author; Email: a.dahia@crnb.dz, dahia.univ@gmail.com

Article Info

Article history:

Received March 23,2022
Revised May 30, 2022
Accepted June 15, 2022

Keywords:

CFD
VOF
Jet breakup
Drop size
Intact length

ABSTRACT

The present paper consists of a numerical investigation carried out for primary break up analysis of a vertical water jet. Many parameters impact the flow development such as velocity, turbulence and nozzle shape. In this work, two types of nozzle geometries have been performed, the first is a capillary circular and the second is conical. The calculations have been performed using the CFD Code Fluent of ANSYS, considering laminar and turbulent flow regimes. While turbulence was modelled using RNG k-ε of RANS approach. The main results show that the jet evolves differently in the two considered nozzle geometries comparing the jet intact lengths, drop sizes and distance between successive drops. It is observed that the turbulence increases substantially the jet intact length and enables the jet breakup at the lower part of the water column. For the conical nozzle case, the jet instabilities grow quickly resulting a drop size in the same order of the jet diameter and an intact length larger in comparison with the circular nozzle case.

I. Introduction

Liquid jets of a free flow are considered naturally unstable. The growth instabilities are the main contributor to the breakup of the jet into droplets of various sizes. This phenomenon is of a great interest in the industrial processes and natural environment. The breakup process is fundamental in nuclear industry for the development of improved injection system in PWR (Pressurized Water Reactor), drug fabrication, impression with ink-jet and pulverization systems aircraft industry, such as turbojets and rocket motors combustion.

The most important studies are concentrated on the breakup behaviour under several factors effect, such as the surface tension, aerodynamic interaction effects, liquid turbulence at the nozzle exit, velocity profile relaxation, and the cavitation. It was important for scientists to understand and characterize the physical phenomena which develop at the interface of the two fluids (jet liquid – surrounding gas), and which ensure the coalescence or breakup of a liquid column. In fact, many studies have been carried out to treat different aspects of liquid jets primary breakup phenomenon in still gases.

According to the bibliography, Rayleigh has showed that the jet breakup is a consequence of hydrodynamic instabilities, liquid viscosity and gravity [01]. It was confirmed that the circular liquid jet is unstable and disturbances are of a wavelength larger than the circumference, the breakup occurs downstream of the nozzle and droplets formed have a size larger than the jet diameter. Sallam et al. [02] have performed an experimental investigation, at standard conditions of temperature and pressure, focused on the liquid column surface. They have defined the primary breakup, the fully dispersed flow regions and the liquid breakup properties, such as droplets sizes and velocities. Ahmed et al. [03] have studied the effect of the velocity profile relaxation on the liquid jet instability in laminar regime out of tubes. They have found a substantial evidence to indicate that the result of the

velocity profile relaxation is similar to the result of relative motion between the jet and its ambient gas, the jet velocity increases and the intact length increase simultaneously. Lebas et al. [04] have used a Direct Numerical Simulation (DNS) for two-phase flows to predict the deformation of liquid jets primary breakup and atomization with high Weber and Reynolds numbers. The model was tested with experimental data. The results have been positively applied in the dense zone of the spray. Cinnella et al. [05] have carried out an important preliminary study to understand the disassociation mechanism of non-axisymmetric free jets. The obtained results give a significant reduction of the breakup length for the square jets. These phenomena seem related to the appearance of a secondary flow, where its intensity develops with the jet speed and promotes its instability.

From this review, it was important to modelling the intact length because it defines the region where the primary breakup is located and the fully dispersed multiphase flow region where should be appear. In addition, to define the drops form, their size and velocity, various parameters should be taken into account including nozzle geometry effects which lead to different velocity relaxation profiles and turbulence at the nozzle exit.

The present study provides a numerical simulation of free water jet surrounded by air. The calculations have been performed using Volume of Fluid (VOF) method. This technic has an advantage of being conceptually simple, reasonably accurate in the interface detection. The investigations allow the detection of the different breakup modes according to different flow conditions. The effect of the main parameters, such as flow velocity, turbulence and the nozzle shape for two form of nozzle geometries have been performed; the first one is a circular and the second is conical.

Therefore, our goal is to demonstrate the sensitivity of the nozzle geometry characteristics on the liquid jet, near field liquid jet characteristics, and flow behaviour to the differences in the change of ejection angles. This work is focused towards the visualization of the water-jet profile behaviour after discharge into the surrounding ambient still air from pressure nozzle, and to determine the breakup length. This study can identified the dependence the atomization of the liquid jet with diverse criteria, such as:

- The disturbance of the surface flow caused by surface tension,
- The effect of the water forces, which favors the detachment of the flow from the nozzle walls,
- The generation of cavitation, inertia forces, and viscous forces which reduces the water jet intact length ..etc.

The numerical results have been compared against experimental data of Sallam et al. [02] and Shengyon et al. [06]. It has shown that the fundamental parameter responsible of the disintegration of the water jet is the instability caused by the surface tension. However, other parameters can modify the breakup process and the droplets size distribution. These include aerodynamic forces, velocity profile relaxation, and the turbulence intensity.

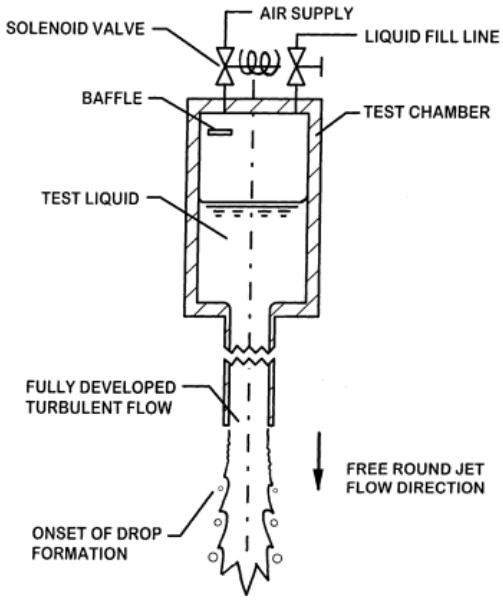

Figure 1. Turbulent liquid jet device used in the experiment of Sallam et al. [02].

II. Mathematical modelling

II.1. Momentum equations

The water jet breakup process was simulated basing on a mathematical model implemented in the CFD code Fluent of Ansys. This model is based on Finite Volume method to solve the entire computational domain for an incompressible Newtonian fluid in axisymmetric geometry. The momentum equation for computational domain is written as:

$$\nabla . U = 0 \quad (1)$$

$$\frac{\partial \rho U}{\partial t} + \nabla . \rho U = -\nabla p + \nabla . (\mu \nabla U) + \rho g + F_{sv} \quad (2)$$

Where, g and p are the gravity acceleration and pressure, respectively. The volume fraction φ of the primary phase, (water in our case) has the following form:

$$\frac{\partial \varphi}{\partial t} + U \nabla \varphi = 0 \quad (3)$$

Whereas φ_{air} is air volume fraction defined:

$$\varphi_{air} = 1 - \varphi \quad (4)$$

In each control volume, the volume fraction of all phases sum to unity. The proprieties appearing in the transport equation namely density ρ and the viscosity μ of the mixture are defined by a linear weighing of both water and air density and viscosity respectively, are deduced from equations 5 and 6:

$$\rho = \rho_{air}(1 - \varphi) + \rho_w \varphi \quad (5)$$

$$\mu = \mu_{air}(1 - \varphi) + \mu_w \varphi \quad (6)$$

In the developed method of Brackbill. [07], the continuum surface force (CSF) method replaces the requiring to define the exact location of the free surface by converting the surface tension into an equivalent volume force. It is coupled to momentum equations as an additional body force. This force acts only in a finite transition region across the interface, which contains the interfacial and their immediate neighboring cells. It is determined by the following expression:

$$F_{sv} = \sigma \frac{\rho_w}{\frac{1}{2}(\rho_{air} + \rho_w)} k \nabla \varphi \quad (7)$$

Where σ is the free surface tension. $\nabla\varphi$ and k are defined as the water volume fraction gradient and the air–water interface curvature respectively.

$$k = -\nabla n \quad \text{and} \quad n = \frac{\nabla \varphi}{\|\nabla \varphi\|} \quad (8)$$

Although it is known that turbulence near interfaces separating two immiscible fluids can be strongly anisotropic involving rapid and complex deformations, breaking, and merging. In this study, for the simplicity and practical computing time, the standard k–ε turbulence model is adopted.

II.2. Turbulence modelling

The eddy viscosity is obtained by solving a set of turbulence transport equations. The two equations of k-ε model is a first-order model based on the turbulent viscosity assumption of Boussinesq. These models are based on an assumption that corresponds to an arrangement between Reynolds stress tensor and mean strain tensor. For two-

equation models, the turbulent viscosity is expressed as function of two quantities such as kinetic energy k and dissipation ε (Eqs. 9 and 10) [8].

$$\begin{cases} \frac{Dk}{dt} = \frac{\partial}{\partial x_j}\left[\left(\nu + \frac{\nu_t}{\partial_k}\right)\frac{\partial k}{\partial x_j}\right] + P_k - \varepsilon - D \\ \frac{D\varepsilon}{dt} = \frac{\partial}{\partial x_j}\left[\left(\nu + \frac{\nu_t}{\partial_\varepsilon}\right)\frac{\partial \varepsilon}{\partial x_j}\right] + c_{\varepsilon 1} f_1 \frac{1}{T_t} P_k - c_{\varepsilon 2} f_2 \frac{\varepsilon}{T_t} + E \end{cases} \quad (9)$$

Where P_k is the production of turbulent kinetic energy given by: $P_k = -\overline{u_i u_j}\frac{\partial U_i}{\partial X_j}$

The eddy viscosity ν_t in k-ε model is calculated by combining k and ε:

$$\nu_t = C_\mu f_\mu k^2/\varepsilon \quad (10)$$

Where C_μ is a constant, f_μ being the damping function. T_t is a turbulence time scale. ε is the modified isotropic dissipation rate. D and E are near wall correction functions for k and ε equations, respectively.

It's noticed that there is no source term in the kinetic energy and the calculation is similar to a single-phase turbulence calculation. The model constants in low Reynolds number are; C_μ=0.09, $C_{\varepsilon 1}$= 1.44, $C_{\varepsilon 2}$=1.92.

III. Numerical modelling and boundary conditions

In order to perform the numerical investigations, two configuations of different nozzle shapes have been considered. In the first case, the nozzle shape is circular without contraction angle (α=0°), however, in the second one, the nozzle has a conical shape with a contraction angle (α) of 8°. The contraction angel (α) represent the angle between the jet axis and the nozzle walls (Fig. 2).

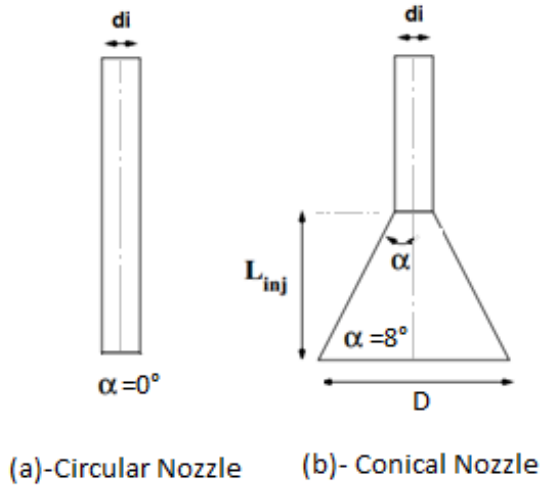

Figure 2. nozzles geometries used in the simulation.
(a) circular nozzle (α=0°), (b) conical nozzle (α=8°).

The considered geometry in the simulations is represented in Figure 3, it is a two dimensional configuration, where the calculations domain was limited by different boundary conditions in order to predict the appropriate jet behavior. At the inlet, a uniform velocity profile is considered, the injection velocity is imposed and water volume fraction is set equal to 1. At the duct wall, no slip condition for the fluid was applied. The upper, lower and lateral sections of the domain are modelled as a Pressure-Outlet boundary condition. As the computational domain is reduced, a symmetry boundary condition is consequently used at symmetry planes.

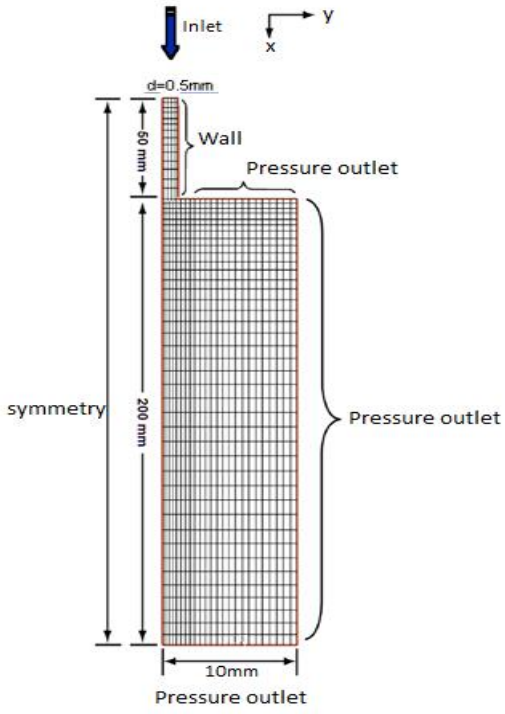

Figure 3. Schematic diagram of the computational domain and boundary conditions.

Therefore, to give reproducible results and to ensure mesh independence, comparative calculations were conducted for different meshes to select the most suitable. This calculations were based on simulations carried out with 08 (eight) different quadratic mesh grids in two dimensional rectangular domain. Figure (4) represents the mean longitudinal velocity for the different considered grids, the grid sensitivity has tackled the axial grid arrangement (Fig. 4a), and the radial grid arrangement (Fig. 4b). The results show that the grid 670x50 is the most suitable for rest of the calculations.

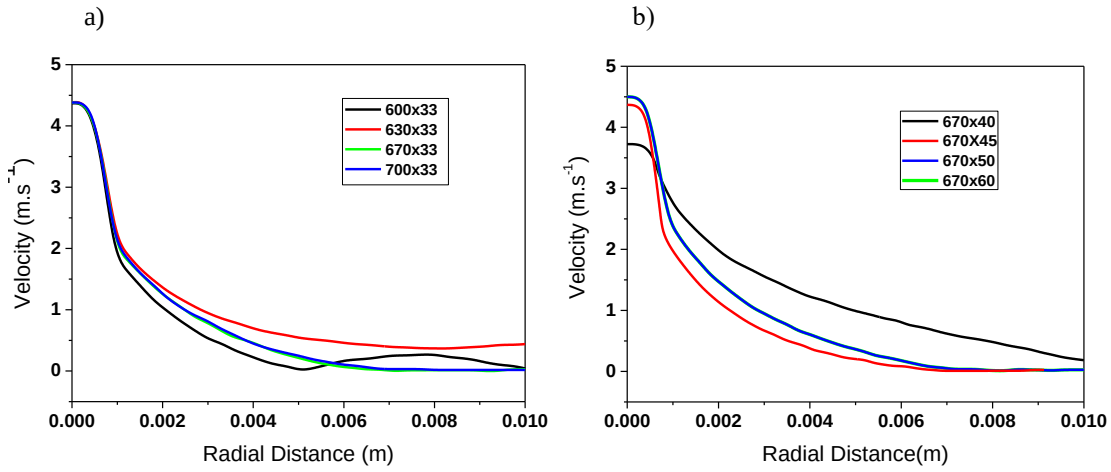

Figure 4. Axial and radial grid sensitivity, represented by the mean longitudinal velocity.

For the flow parametres and conditions are summarized in Table 1, where the vertical axisymmetric water jet of a density ρ_L is considered, it flows through the air phase at rest, leaving a circular nozzle diameter d_i with a velocity U_i, which is considered variable according to the flow regime, laminar or turbulent. The injection velocity imposed at the exit of each geometry nozzle. The interface was captured with algebraic VOF method. The semi-implicit method for pressure linked equations (SIMPLE) algorithm is used to resolve the partial differential equations [9], [10]. The global current number is less than 0.25 in all cases, and the calculations are made with uniform time steps, which lead to residuals of all calculated variables less than 10^{-6}.

Table 1. Flow parametres characteristics.

Parameter	Range
Liquid	Water
Initial jet diameter (di)	0.5, 1.9, 4.8 and 8.0 mm
Jet exit mean velocity (U_i)	1 to 25 m.s^{-1}
Liquid/gas density ratio (ρ_L/ρ_G)	860
Jet exit Reynolds number (Re)	5000-200 000
Jet exit Weber number (We)	235-270
Normalized liquid jet length (Lc/d)	50-300

IV. Results and discussions

The results presented in this work are obtained by the numerical simulation of a vertical water jet evolving in air at rest. Two configurations with different nozzles shapes were chosen according to their contraction angle. The investigations were concentered on the intact length evolution against jet velocity, the influence of nozzle shape on the jet behaviour, the impact of velocity relaxation profile and turbulence on the jet breakup phenomenon. The results were compared to the measurements of Sallam et al. [02] and Shengyon et al. [06].

IV.1. Water free jet morphology

The general form of a free water jet is designed from an intact length, which is the distance from the nozzle exit to the first drop appeared, and the drops of diameter greater than the jet diameter. The jet intact length can be easily identified from the nozzle exit until the first spike appearance (Fig. 5a, Point A). The obtained results by numerical simulation show that, the VOF model reproduce correctly the free jet breakup phenomenon. According to Figure 5(b), the water jet breakup has occurred from an intact length, estimated at 18 mm from the nozzle exit. The formed droplets are larger than the jet diameter *(=1.9d_j)*. This corresponds to the first breakup called "Rayleigh regime", where the breakup has mainly occurred due to the surface tension force. A surface waves will be created and amplified along the jet axis, reaching a sufficient amplitude then fevors the jet to breakups into drops.

For a better description, the volume fraction distribution of water phase along the jet axis is presented in Figure 5(b). The breakup of liquid jet takes place at the position where the water volume fraction is zero, and the drops diameter is therefore represented by the points thickness.

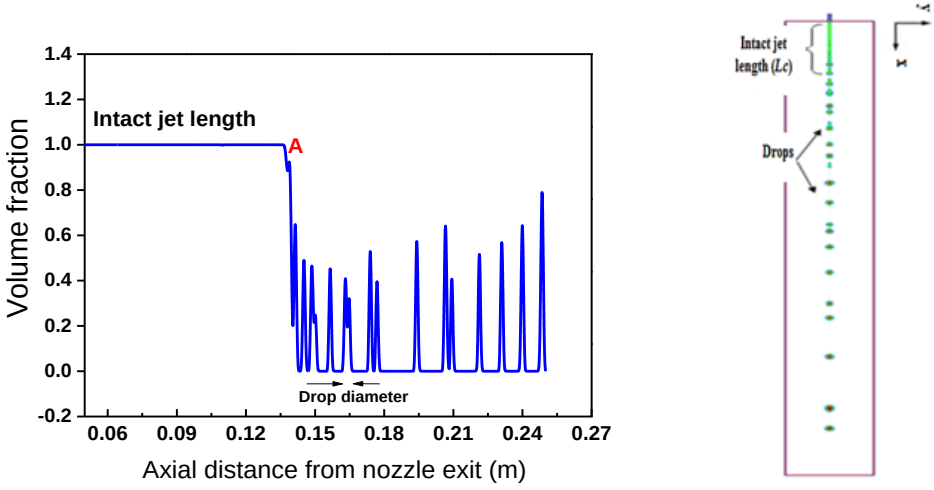

Figure 5. Free water jet phenomenology for a circular nozzle (α=0°) and laminar flow.
(a) evolution of the water volume fraction on the jet axis.
(b) water jet breakup into drops by cfd-fluent simulation.

In Figure 6, a harmonic fluctuation of the jet velocity along the symmetry axis is shown. For laminar flow, the water column is not disturbed before the breakup, the jet velocity is still constant ($U=1.5m.s^{-1}$). The velocity fluctuation along the symmetry axis represent the water droplet velocity and therefore the velocity of the jet after breakup [11], [12], [13]. Although, in the VOF model the relative velocity in the interface between the air and water is considered zero. This assumption did not affect the cells far from the considered interface.

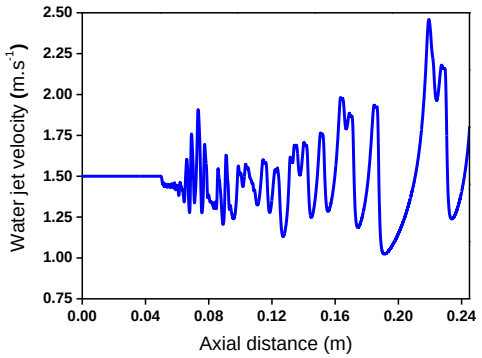

Figure 6. Water jet velocity fluctuation along the water jet axis for laminar flow regime.

From velocity vectors in Fig. 7, water drops could be localised in the regions of high intensity. The figure also describes the velocity evolution along the jet axis and around the water drops over the computational domain.

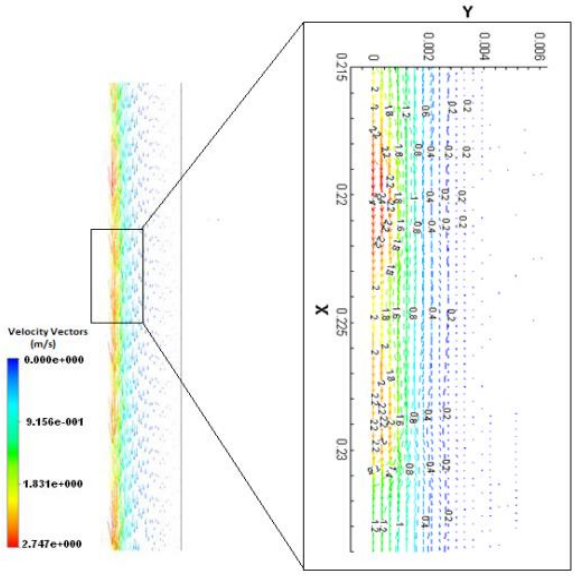

Figure 7. Velocity vectors in the flow domain.

For a turbulent flow of *Re=5030* and *We=235*, a comparison is performed between numerical results and experimental data of Sallam et al. [2], Figure 8. Qualitatively, a good agreement is recorded in terms of droplets size. However, some discrepancies are observed about the intact length. In fact, a nozzle length of $L_{inj} = 10d_i$ was considered, it was chosen arbitrarily because the authors Sallam et al. [2] did not report the nozzle length used in the experiment. This finding is attributed to the nozzle length affect, which affect the breakup process because the development of the velocity profile along the jet nozzle length.

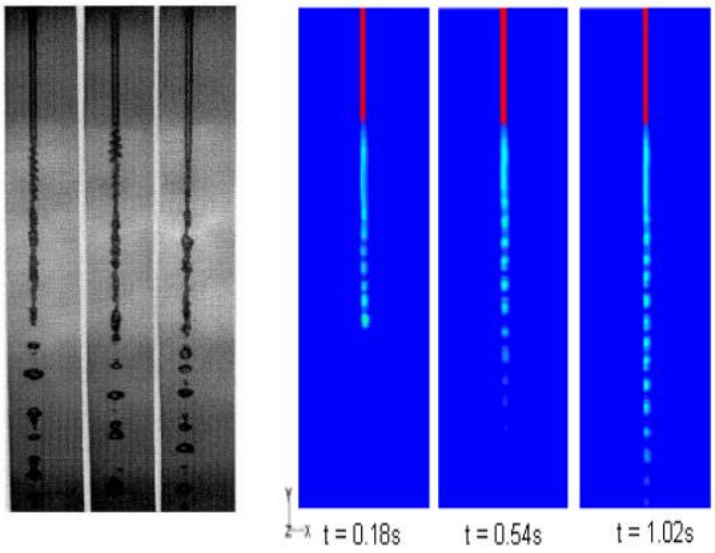

Figure 8. Turbulent circular jets; d=1.9mm, *Re=5030, We=235*
a) experience of Sallam et al., (2002), b) VOF simulation.

IV.2. Intact jet length evolution

In order to study the jet intact length evolution, two geometries of circular nozzles were considered with different diameters of 6.8mm and 8.4mm respectively. Some typical comparisons with the experimental data of Shengyon et al. [6] are illustrated in Figure 9. The numerical results are in good agreement with the experience with an average error of approximately 14% and 7% respectively. For both diameters, the jet intact length, in laminar flow, increases while increasing velocity, then it decreases when the jet velocity exceeds a critical value (Fig. 9a). When the flow reaches a fully turbulent regime, the intact length continue to increase with velocity without a remarqued critical point (Fig. 9b).

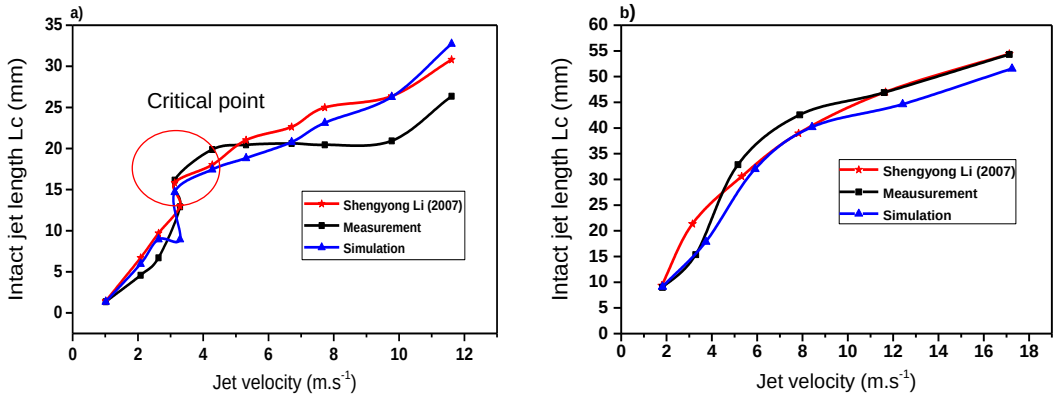

Figure 9. Intact jet length evolution as function of the jet velocity,
(a) *di=6.8mm*, (b) *di=8.4 mm.*

According to the experimental data, the low velocity (creeping mode) allow drop formation at the immediate nozzle exit, this range of flow regime was not taken in consideration for this work. When the injection velocity increases above ($U \simeq 1\ m.s^{-1}$), the intact length begins to appears (see Figure 9); this is the beginning of the second region called "Rayleigh mode". In this region, the intact length increases linearly with the flow velocity ($U \simeq$ *1-1.5* $m.s^{-1}$), which is independent of the velocity relaxation profile. Hence, the breakup is completely controlled by capillary or surface tension force [14].

When the jet velocity increases from 2.5 to 7.5 $m.s^{-1}$, the intact length increases simultaneously then become uniform. The surface tension force, which has a mitigating effect, tend to reestablish the original shape of the liquid column after disturbance [15]. Hence, the conical nozzle shape (α=8°) modifies significantly the behavior of the

jet, and the water column breakup can be distinguished further downward of nozzle causing an intact length, *Lc*, more important (example, at $U = 2\ m.s^{-1}$), $Lc = 124.14\ mm$), (Fig. 10). In the transition zone ($U > 2\ m.s^{-1}$), the intact length decreases with the jet velocity. The two regions (increase then decrease) are connected by a "critical point", which represent the critical velocity where the stability curve shows a maximum. The critical point location depends strongly on the initial injections conditions [16] and changes with the nozzle length. Beyond $U \simeq 4.5\ m.s^{-1}$, the flow was considered turbulent, and the intact length increases again. The relative velocity between these two phases favors the water column to breaks. After the second critical velocity, the intact length decreases then starts to increase again (Fig. 10).

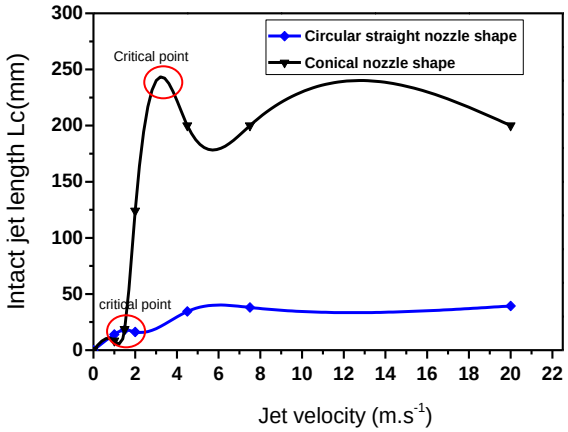

Figure 10. Stability curve of a capillary circular nozzle (α=0°), and conical nozzle shape (α=8°).

For a better visualization of the free jet flow, the velocity streamlines evolution at the exit of the injection nozzle gives a good illustration (Fig. 11). We can see that the water jet draws the surrounding air, initially at rest, while the flow of air around the jet reduces the relative velocity between water and air phases.

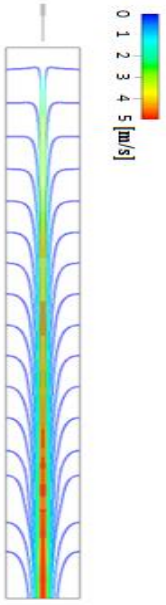

Figure 11. Streamlines evolution in the whole domain of the flow.

IV.3. Drops distribution

The drops distribution for the two nozzle configurations are presented in Figure 12 and 13. Figures (12a) and (13a) describes the laminar regime (U=1 m.s-1), where a uniform drops size was found at the exit equal to the double of the jet diameter (dd =2di) [17]. These observations are similar to those observed in the first Rayleigh regime. However, the distance between two successive droplets increases and becomes non-uniform when the jet moves downward. Otherwise, the turbulent water jet in Figs. 12(b) and 13(b) is noticeably different; the intact jet length is stretched and the distance between two successive droplets is not uniform. Consequently, different drops sizes are observed along the jet axis. The growth of the intact jet length according to the intensity of turbulence is also noticed in the experimental tests of Sallam et al. [2], and described by Ehsan and Ali. [18]. However, the small waves existing on the turbulent jet surface affect the fragmentation of water column and the secondary breakup regime could not be reproduced in the simulation. In this case, a large scale of the simulation (meso-scale simulation) will be adopted.

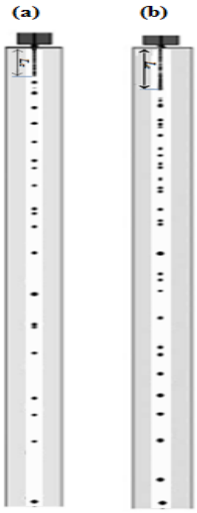

Figure 12. Jet breakup for circular nozzle shape (0°)
a) laminar jet, $U=1\ m.s^{-1}$,

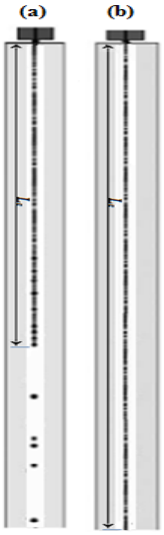

Figure 13. Jet breakup for conical nozzle shape (8°)
b) turbulent jet, $U=20\ m.s^{-1}$.

IV.4. Velocity Profile Relaxation Influence

To investigate the effect of velocity profiles relaxation inside the capillary circular nozzle on the breakup process, numerical simulations were performed for five (05) different lengths of nozzles ranging from 10 to 40 mm (Fig. 14). The calculations tests are performed at a relatively low jet velocity ($U = 1.5\ m.s^{-1}$). As results, the numerical finding show that the intact length of the jet increases with increasing the nozzle length. This conclusion is principally due to the internal jet flow behavior, and the development of the velocity profile inside the nozzle, which affect significantly the breakup of water column. The rearrangement of the jet velocity profile downward of the nozzle exit, and the flat profile explains the higher *Lc* values (Fig. 14).

Contrariwise, when the jet leaves the nozzle with a relatively parabolic profile, the intact length decreases significantly with the nozzle length (50mm nozzle case). This modification in the profile, accompanied by the energy redistribution, contributes significantly to the development of disturbances on the jet surface and the formed ligaments fractionate under the aerodynamic instabilities forces. This fact explains the jet breakup occurred at a short distance downward of the nozzle exit (*Lc= 18.01 mm*). In addition, no circulation zone has been observed inside the tube. All these conclusions, are similar to the findings reported by Ghassemieh et al. [12] and Bode et al. [19].

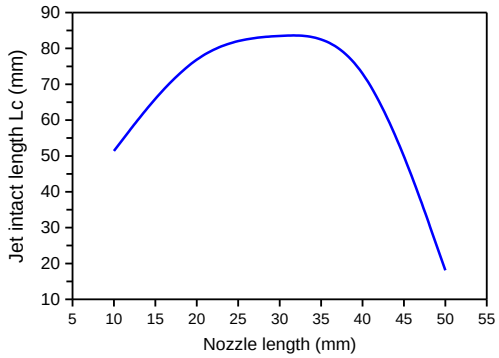

Figure 14. Nozzle effect length on the breakup for low velocity injection value ($U=1.5\ m.s^{-1}$).

For a conical nozzle shape (Fig. 15a), the velocity have a relatively parabolic profile inside the nozzle and the flow patterns are substantially modified at the nozzle exit. Figure 15(b) illustrate how the downstream air is being circulated between the water flow and the nozzle wall. As we indicated previously, the air is entrained in the water flow direction, which generates a downward motion. Consequently, an upward motion of air was formed, this to satisfy the mass conservation [20]. Such effect has not been observed in the capillary circular nozzle configuration.

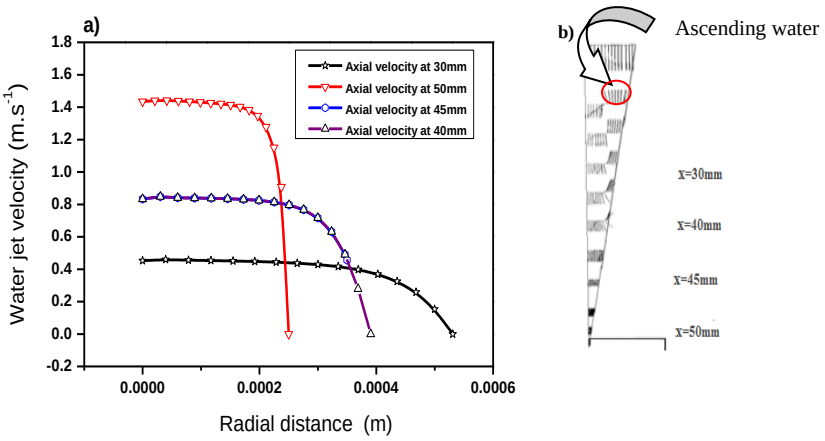

Figure 15. (a) Velocity profile evolution with radial distance (conical nozzle shape), b) Standardized velocity vectors.

IV.5. Turbulence Effect on the Jet Breakup

The turbulence kinetic energy and the growth of disturbances are the main cause of the fragmentation of the liquid jet column into droplets with different sizes [20], [21]. The development of the jet column surface remained dominant and became the main contributor of spray formation. The turbulence kinetic energy is more concentrated in the midline of the jet column (Fig. 16). In case of circular nozzle shape (Fig. 16a), the distortion of the liquid surface by turbulent eddies gives sufficient turbulent energy to supply the surface tension and sufficient time for drops formation. An intact length was clearly developed, and the droplets have a diameter greater than the nozzle exit. This, correspond to the Rayleigh breakup regime. Thereafter, the drops take more time to develop and their size growth progressively with increasing distance downstream of the nozzle exit [22], [23].

In the conical nozzle shape case (Fig. 16b), the downstream air close to the water surface was entrained by the flow and a downward motion was obtained [24]. At the end of the column jet, the instabilities begin to appear, the intact length is infinite and no droplets are formed yet.

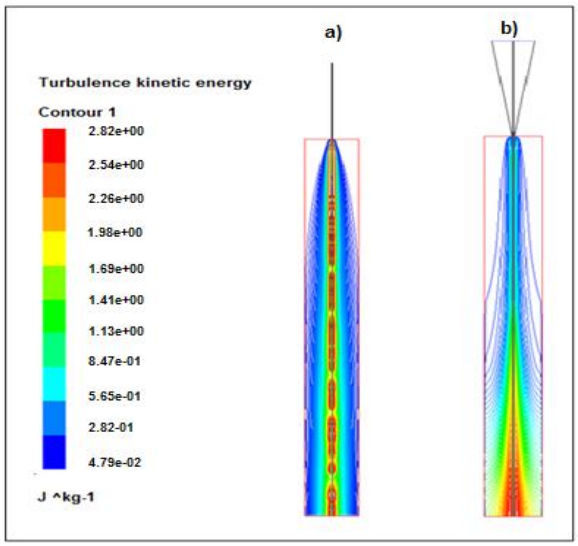

Figure 16. Iso-contour of turbulence kinetic energy.
a) capillary circular nozzle shape, b) conical nozzle shape.

III. Conclusion

In this work, a set of numerical simulations were performed using Volume Of Fluid (VOF) approach available in the CFD Code Fluent. The main objective of the study is to analyses the breakup phenomenon of a liquid column jet according to different parameters, such as nozzle geometry, flow pattern and velocity profile relaxation, which affect directly the flow behavior. Two nozzle configurations were adopted in this work, considering laminar and turbulent flow conditions; the first is circular and the second is conical.

The numerical results show that VOF model has qualitatively reproduces the first jet breakup mode, the size of the drops obtained, is in compatibility with the experimental observations (Rayleigh mode). The gradual increase in jet velocity causes the increase an intact length. These results draw the shape of free liquid jets stability curve and describe the evolution of the intact jet length as function of velocity.

As observed in the experimental data presented in the literature, the introduction of turbulence in the flow modifies the breakup mode compared to that observed in the laminar flow. A further disturbance in the liquid/gas interface is observed.

Consequently, we can conclude that there are various factors that contributes to the breakup of the free water jet in still surrounding air.

For future investigations, model improvements are needed to take into account the turbulence at the water-air interface. For very high flow rates, the development of a more elaborate method that takes into account the relative velocity between the two phases should be examined.

Acknowledgements

This work was supported by funding from Nuclear Research Center of Birine/ Algerian Atomic Energy Commission (COMENA). The authors are grateful thank the Laboratory of Aeronautics Science of Blida University that framing and help us to prepare this study.

References

[1] P. G. Drazin and W. H. Reid, "Hydrodynamic stability," *Cambridge University Press*, 2nd edition: (pp. 626). ISBN: 0-521-52541-1, 2010. https://doi.org/10.1017/CBO9780511616938.

[2] K A. Sallam, Z. Dai, G. M. Faeth,"Liquid breakup at the surface of turbulent round liquid jets in still gases," *International Journal of Multiphase Flow*, Vol. 28, N° 1, pp. 427 – 449, 2002.

[3] M. Ahmed, A. Amighi, N. Ashgriz, H. Tran, "Characteristics of liquid sheets formed by splash plate nozzles," *Exp Fluids*, Vol. 44, pp. 125 – 136, 2008.

[4] R. Lebas, T. Menard, P. A. Beau, A. Berlemont, F. X. Demoulin, "Numerical simulation of primary breakup and atomization: DNS modeling study," *International Journal of Multiphase Flow*, Vol. 35, N° 3, pp. 247 – 260, 2009.

[5] P. Cinnella, P. Luciana, L. Domenico, "Comparison of the stability properties of round and square liquid jets," Conference paper, *59th annual congress ATI*, 2004, Geneva.

[6] L. Shengyon, L. Mouwei, Z. Shaojun, Z, "Study on the breakup length of circular impinging jet, Mechanical Engineering School," *Journal of University of Science and Technology*, Beijing-China, Vol. 14, N° 6, pp. 585, 2007.

[7] J. U. Brackbill, D. B Kothe, C. Zemach, "Continuum method for modeling surface tension," *J. Comput. Phys*, Vol. 100, pp. 335–354, 1992.

[8] S. Gorji, M. Seddighi, C. Ariyaratne, A. E. Vardy O'Donoghue, T. D. Pokrajac, S. A. He, "comparative study of turbulence models in a transient channel flow," *Journal of Computers & Fluids*, Vol. 89, pp. 111–123, 2014.

[9] V. Ambethkar, "Numerical study of coupled fluid flow with heat and mass transfer using finite volume discretization," *Journal of Mathematical and Computational Science*, Vol 5, No 1, pp. 99-122, 2015.

[10] S. V. Patankar and D. B. Spalding, "A calculation procedure for heat, and momentum transfer in three-dimensional parabolic flows," *Int. J. Heat Mass Transf*, Vol. 15, pp. 1787 – 1806, 1972.

[11] A. Chauhan, C. Maldarelli, D. S. Rumschitzki, D. T. Papageorgiou, "An experimental investigation of the convective instability of a jet,"*Chemical Engineering Science*, Vol. 58, pp. 2421 – 2432, 2003.

[12] E. Ghassemieh, H. Verstee, M. Aca, "The effect of nozzle geometry on the flow characteristics of a small water jets," *Proceeding of the IMechE Part C: Journal of Mechanical Engineering Science*, Vol. 220, N° 12, pp. 1739 – 1753, 2006.

[13] G. Hermann and A. Michalke, "On the inviscid stability of a circular jet with external flow," *J. Fluid. Mech*, Vol. 114, pp. 343 – 359, published in 2006. DOI: https://doi.org/10.1017/S0022112082000196.

[14] T. Menard, S. Tanguy and A. Berlemont, "Coupling level set/vof/ghost fluid methods: Validation and application to 3D simulation of the primary break-up of a liquid jet," *International Journal of Multiphase Flow*, Vol. 33, N° 5, pp. 510–524, 2007. https://doi.org/10.1016/j.ijmultiphaseflow.2006.11.001.

[15] S. P. Lin and R. D. Reitz, "Drop and spray formation from a liquid jet," *Annual Review of Fluid Mechanics*, Vol. 30, N° 1, pp. 85 – 105, 2003.

[16] J. B. Blaisot and S. Adeline, "Instabilities on a free falling jet under an internal flow breakup mode regime," *International journal of Multiphase flow*, Vol. 29, N° 4, pp. 629–53. 2003.

[17] S. P. Lin and R. D. Reitz, "Drop and spray formation from a liquid jet," *Annual Review of Fluid Mechanics*, Vol. 30, N° 1, pp. 85 – 105, 2003.

[18] F. Ehsan and D. Ali, "Numerical simulation of the breakup of elliptical liquid jet in still air," *J. Fluids Eng*, Vol. 135, N° 7, 071302, 2013.

[19] M. Bode, F. Diewald, D. Broll, J. Hesyse et al., "Influence of the injector geometry on primary breakup in diesel injector system," *SAE Technical Paper*, 2014-01-1427, 2014.

[20] T. Vahendi, B. Pourdeyhim, "The effect of nozzle geometry on waterjet breakup at high Reynolds numbers," *Experiments in fluids*, Vol. 35, pp. 364–371, 2003. DOI: 10.1007/s00348-003-0685-y.

[21] M. Sylvain, "Contribution à l'étude de l'atomisation assistée d'un liquide, instabilité de cisaillement et génération du spray," *Doctorat thesis*, 2015, Grenoble University- France.

[22] K. Sallam, C. Ng, R Sankarakrishnan, C. Aalburg and K. Lee "Breakup of turbulent and no-turubulent liquid jets in gaseous crossflow," 44th AIAA Aerospace Science Meeting and Exhibit, Reno, Nevada, AIAA-2006-1517, 2006, pp. 9-12. https://doi.org/10.2514/6.2006-1517.

[23] M. Movassat, N. Maftoon and A. Dolatabadi, " A Three-Dimensional Numerical Study of the Breakup Length of Liquid Sheets," *in Proceedings of the 21st Annual ILASS-Americas Conference*, Institute for Liquid Atomization and Spray Systems, Orlando, Florida, May 2008.

[24] T. Yeng-Yung, L. Cheng-Yen, L. Shi-Wen, L, "Coupled Level-set and Volume-Of-Fluid method for two-phase flow calculations," *Num. Heat Tran J. Part B*, Vol. 71, N° 2, pp. 173-185, 2017. http://dx.doi.org/ 10.1080/10407790. 2016.1265311.